Int. J. Heat Mass Transfer. Vol. 5, pp. 457–468. Pergamon Press 1962. Printed in Great Britain.

RADIATIVE HEAT-TRANSFER CALCULATIONS FOR INFINITE SHELLS WITH CIRCULAR-ARC SECTIONS, INCLUDING EFFECTS OF AN EXTERNAL SOURCE FIELD

MAX A. HEASLET and HARVARD LOMAX

National Aeronautics and Space Administration, Ames Research Center, Moffett Field, Calif.

(*Received* 21 *September* 1961)

Abstract—Diffuse radiation from infinite shells with circular-arc cross-sections is analyzed for cases involving external source fields of either diffuse or parallel radiation. The governing integral equations are derived under conditions corresponding to a modified grey-body analysis, and the inversions given in closed form. Specific applications provide local heat transfer corresponding to constant shell temperature, local temperature corresponding to constant heat transfer, and predictions of equilibrium temperatures when the shell is a thermal shield. Comparisons are made with similar calculations for hemispherical shields.

NOMENCLATURE

$B(\theta)$, $B_0(\theta)$, $B_1(\theta)$, $B_2(\theta)$,	radiation-flux functions (energy per unit time and area) introduced in equations (1);
e_d,	flux of diffuse radiation from external source;
e_s,	flux of parallel radiation from external source;
dF_{1-2},	incremental shape factor, equation (2);
$h_2(\theta)$, $H_1(\theta)$, $H_2(\theta)$,	flux of incident radiation introduced in equations (1);
$Q(\theta)$,	local heat-transfer function, equation (5a);
R,	radius of circular cross-section of shell;
$T(\theta)$,	temperature distribution;
T_E,	equilibrium temperature;
$Z_n(\gamma, \psi)$,	function in equation (15).

Greek symbols

α,	absorptivity;
ϵ,	emissivity;
θ,	angular co-ordinate of point on circular arc (see Fig. 1);
σ,	Stefan–Boltzmann constant;
ψ,	angle fixing extent of circular arc (see Fig. 1).

INTRODUCTION

INTEREST in radiative cooling of space vehicles, solar-energy collectors and thermal-radiation shields has brought about a need to increase the fund of engineering knowledge through predictions of the characteristics of basic geometric configurations and through application of available mathematical techniques to the analysis of the fundamental equations. The present paper is intended to contribute to this fund. Firstly, a simple geometry is studied involving diffuse reflection and emission from a heated cylindrical shape with circular-arc cross-section that may also be receiving radiation from an external source. Secondly, the inversion of the governing integral equation is presented explicitly in terms of a single integration formula. In spite of the simplicity in concept and execution, no previous developments of this sort appear to have been carried out.

The study of radiative transfer is intimately related to the study of integral and integro-differential equations. Continuing improvements in high-speed computing equipment and advances in programming methods have eased greatly the logistic demands in the attack on such problems. The following analysis is, in fact, an outgrowth of a detailed, numerical study of thermal radiation near the junctures of heated and interacting surfaces. It became apparent during the study that, for a single curved surface of circular-arc cross-section, no recourse to numerical methods was necessary. The results to be given can actually be generalized analytically even further, to include sections of arcs and monochromatic radiation. In order to limit the number of parameters, however, dependence on wavelength has been suppressed and single arcs are considered.

We confine ourselves to the equilibrium radiant interchange of energy between an infinitely long shell of circular-arc cross-section and an external black-body source field. Additional conditions, such as given temperature or heat transfer along the walls of the shell, will be introduced later. For example, radiation from the convex side can be removed from the problem and in this case the radiation along the concave portion corresponds to the emission and reflection from within a groove on the surface of a body. Both emission and reflection will be assumed diffuse and the material of the shell opaque. A grey-body type of analysis will be used, i.e. the coefficients of emission, absorption, and reflection are to be independent of temperature and frequency *except* that two extreme temperature and frequency ranges with separate coefficients will be admitted. In this way we shall account for possible differences between the emissivity or absorptivity in the relatively low-temperature regime of the walls and the absorptivity of the incident external energy which may come from a source of much increased temperature, as, for example, in the case of solar radiation.

The next section derives the governing equations and then shows how the basic integral equation with known kernel can be inverted. The final section applies the theory to four problems of practical interest.

GOVERNING EQUATION AND GENERAL SOLUTION

The energy–flux balance

Figure 1 shows a cross-section of the shell with angular co-ordinates denoting positions of radii drawn through the center of the circular arc. With no loss of generality, the co-ordinates of points on the shell may be measured from the radius that bisects the cross-section, positive values denoting a counter-clockwise rotation. Let $B(\theta_1)$ be the total radiation flux (energy per unit time and area) from the representative point P_1 with angular co-ordinate θ_1. This flux is calculated by summing two effects: the emission and the reflection.

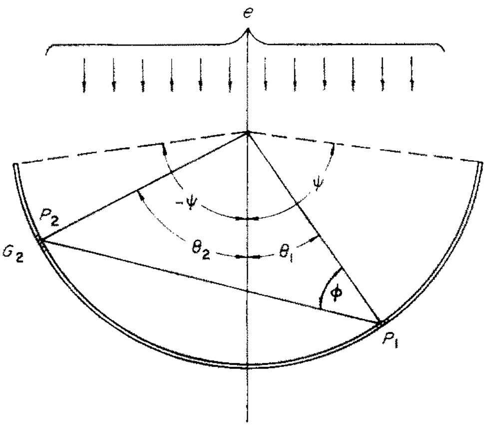

FIG. 1. Co-ordinate system.

Emitted energy flux is given by $\epsilon\sigma T^4(\theta_1)$ where ϵ is grey-body emissivity at the average body temperature, σ is the Stefan–Boltzman constant and $T(\theta_1)$ is the local temperature.

The reflected energy is the difference between the incident and absorbed energy at P_1. In this paper the incident flux at P_1 is separable into two parts: $H_1(\theta_1)$, flux with a certain low-average frequency being emitted and reflected from the concave side of the shell; and flux with a different high-average frequency either coming from the external source, $h_2(\theta_1)$, or being reflected from inside the shell, $H_2(\theta_1)$. All reflection is considered to be diffuse and at the same average frequency as the incident radiation. In order to admit differences between the absorption of incident radiation with widely different spectrums, we introduce two absorption coefficients: α_1 (which is equal to ϵ) and α_2, associated with the average frequency ranges of H_1 and $[h_2, H_2]$, respectively.

The expression for emitted radiant flux is thus

$$B(\theta_1) = B_0(\theta_1) + B_1(\theta_1) + B_2(\theta_1) \quad (1a)$$

$$B_0(\theta_1) = m\sigma\epsilon T^4(\theta_1) \quad (1b)$$

$$B_1(\theta_1) = \sigma\epsilon T^4(\theta_1) + (1 - \epsilon)H_1(\theta_1) \quad (1c)$$

$$B_2(\theta_1) = (1 - \alpha_2)\,[h_2(\theta_1) + H_2(\theta_1)]. \quad (1d)$$

The flux $B_0(\theta_1)$ is to be identified with radiation from the convex side of the shell. Thus $m = 1$ if the rear side is emitting energy, and $m = 0$ if the contribution of this side is to be excluded. The factors $(1 - \epsilon)$ and $(1 - \alpha_2)$ involving the two absorptivities are, respectively, the reflectivity factors, ρ and ρ_2.

The basic governing equations may be derived through the conventional use of geometric shape factors (see, e.g., Jakob [1], p. 6 *et seq.*).

Consider, firstly, the low average-frequency distribution $H_1(\theta_1)$. If at the point P_2 with angular co-ordinate θ_2 an infinitesimal area dS_2 is situated, the incident energy per unit time and area at P_1 that comes from dS_2 with the same average frequency as $H_1(\theta_1)$ is

$$B_1(\theta_2)\, dF_{1-2}$$

where dF_{1-2} is the shape factor of dS_2 as seen from P_1. Once this factor is known, an integration along the cylinder and over the entire arc, from $-\psi$ to ψ yields $H_1(\theta_1)$. It is known, moreover, that the two-dimensional shape factor, applicable to unit length of the cylinder, is

$$dF_{1-2} = \tfrac{1}{2}\, |d(\sin\varphi)| \tag{2}$$

where, as shown in Fig. 1, φ is the angle between the normal to the arc at P_1 and the line P_1P_2 (see Jakob [1], pp. 19–21). For circular arcs

$$\varphi = \frac{\pi}{2} - \frac{(\theta_1 - \theta_2)}{2}$$

and as a consequence one gets

$$H_1(\theta_1) = \frac{1}{4}\int_{-\psi}^{\psi} B_1(\theta_2) \sin \frac{|\theta_1 - \theta_2|}{2}\, d\theta_2. \tag{3a}$$

By an identical argument one finds for the additional (high-frequency radiation) flux functions the relation:

$$H_2(\theta_1) = \frac{1}{4}\int_{-\psi}^{\psi} B_2(\theta_2) \sin \frac{|\theta_1 - \theta_2|}{2}\, d\theta_2. \tag{3b}$$

Equations (1c), (1d) and (3a), (3b) can be combined to form

$$B_1(\theta_1) = \epsilon\sigma T^4(\theta_1) + \frac{(1 - \epsilon)}{4}\int_{-\psi}^{\psi} B_1(\theta_2) \sin \frac{|\theta_1 - \theta_2|}{2}\, d\theta_2. \tag{4a}$$

$$B_2(\theta_1) = (1 - \alpha_2) h_2(\theta_1) + \frac{(1 - \alpha_2)}{4}\int_{-\psi}^{\psi} B_2(\theta_2) \sin \frac{|\theta_1 - \theta_2|}{2}\, d\theta_2. \tag{4b}$$

Equations (4) are the governing integral equations, Fredholm equations of the second kind with kernel

$$\sin \frac{|\theta_1 - \theta_2|}{2},$$

and their solution yields the combined radiative flux in both averaged frequency ranges as a function of θ_1. If both the energy source $h_2(\theta_1)$ and the wall temperature distribution $T(\theta_1)$ are specified, the equations are uncoupled. For such cases the radiation fluxes in the two averaged-frequency ranges are independent of one another. If the temperature along the shell is not given, equations (4a) and (4b) are not independent. They are coupled by the local heat-transfer function $Q(\theta_1)$, defined as the difference between the emitted and absorbed energy per unit time and area. Thus

$$Q(\theta_1) = B_0(\theta_1) + B_1(\theta_1) + B_2(\theta_1) - H_1(\theta_1) - H_2(\theta_1) - h_2(\theta_1) \tag{5a}$$

or, alternatively,

$$Q(\theta_1) = m\epsilon\sigma T^4 + \frac{\epsilon}{1 - \epsilon}[\sigma T^4 - B_1] - \frac{\alpha_2}{1 - \alpha_2} B_2. \tag{5b}$$

Using equations (1), (3), (4) and (5), one can show:

$$\left.\begin{aligned} (m + 1)\,\epsilon\sigma T^4 &= Q + \frac{\alpha_2(1 - \epsilon)}{1 - \alpha_2} h_2 \\ &+ \frac{\alpha_2(\epsilon - \alpha_2)}{(1 - \alpha_2)^2} B_2 + \frac{1}{4}\int_{-\psi}^{\psi} [(m + 1 \\ &- m\epsilon)\,\epsilon\sigma T^4 - (1 - \epsilon) Q] \sin \frac{|\theta_1 - \theta_2|}{2}\, d\theta_2 \end{aligned}\right\} \tag{6a}$$

$$B_2 = (1 - \alpha_2) h_2 + \frac{1 - \alpha_2}{4}\int_{-\psi}^{\psi} B_2 \sin \frac{|\theta_1 - \theta_2|}{2}\, d\theta_2. \tag{6b}$$

If the energy source and the heat-transfer function Q are specified, equations (6a) and (6b) form a pair of simultaneous integral equations for the temperature distribution. Fortunately, however, the solution to (6b) does not depend upon the solution to (6a) and, as shown in a subsequent section, the complete inversion to both equations can be determined.

External radiation source

In this report, the incident radiation from the external source is considered to enter the open face of the arc and to be one of two kinds: e_d, a known flux of diffuse radiation, or e_s, a known flux of parallel rays. The former could be formed by emission from a black body opposite the opening, representative, for example, of a high-temperatured furnace wall. The latter could be an idealization of radiation from a distant sun.

The shape factor of equation (2) also applies to the diffuse radiation e_d, where now the element dS_2 lies along the chord connecting the ends of the arc. For a uniform incident field, $e_d =$ const. $= e_{d_0}$,

$$h_2(\theta_1) = e_{d_0} \cos \frac{\psi}{2} \cos \frac{\theta_1}{2}. \tag{7a}$$

If, on the other hand, the incident radiation is uniform and parallel, $h(\theta_1)$ is the product of e_{s_0} and the cosine of the angle between the inner normal to the surface at P_1 and a vector parallel to the incident rays. If ψ is greater than $\pi/2$, or if the direction of the oncoming radiation is sufficiently askew with respect to the radius that bisects the arc, regions of shadow are formed on the inside. In these regions e_s is, of course, zero. (Similarly, regions on the outside receive radiation if the arc represents a shield.) The analysis of examples representing partially shadowed arcs falls within the scope of the methods of this report but no further attention is given them. For the case when $\psi \leqslant \pi/2$ and the uniform parallel radiation is directed along the plane of symmetry

$$h_2(\theta_1) = e_{s_0} \cos \theta_1 \tag{7b}$$

where e_{s_0} is a constant.

Methods of solution

The previously derived integral equations are various forms of the Fredholm integral equation

$$F(\theta) = G(\theta) + \frac{\mu^2 - \gamma^2}{2\mu} \int_{-\psi}^{\psi} F(\theta_1) \sin \mu|\theta - \theta_1|\, d\theta_1. \tag{8}$$

At the position $\theta = \theta_1$, the kernel of equation (8) has a discontinuity in slope in common with Green's function for ordinary second-order differential equations, and this prompts one to seek a possible re-expression in terms of a differential equation. Twofold differentiation of equation (8) does, in fact, yield an expression that combines with equation (8) to form

$$\frac{d^2F}{d\theta^2} + \gamma^2 F = \frac{d^2G}{d\theta^2} + \mu^2 G. \tag{9}$$

A solution of equation (8) must, therefore. satisfy equation (9) and, conversely, the general solution of the differential equation must contain the solution of the integral equation.

The general solution to equation (9) can be written

$$F(\theta) = C_1 \cos \gamma\theta + C_2 \sin \gamma\theta + I_p(\theta) \tag{10}$$

where C_1 and C_2 are arbitrary constants and $I_p(\theta)$ is the particular integral satisfying the right-hand side of equation (9). The constants C_1 and C_2, although arbitrary for a solution of equation (9), are not so for the solution of equation (8). They were lost in passing from equation (8) to (9) by the double differentiation, but they can be determined if $F(\theta)$, as given by equation (10), is placed into equation (8) and the coefficients of like terms are equated. There results

$$F(\theta) = C_1(\gamma, \mu, \psi) \cos \gamma\theta + C_2(\gamma, \mu, \psi) \sin \gamma\theta + G(\theta) + \frac{\mu^2 - \gamma^2}{2\gamma} \int_{-\psi}^{\psi} G(\theta_1) \sin \gamma|\theta - \theta_1|\, d\theta_1 \tag{11}$$

where

$$\left. \begin{aligned} C_1(\gamma, \mu, \psi) &= \frac{\mu^2 - \gamma^2}{2\gamma} \\ &\times \frac{\gamma \sin \mu\psi \cos \gamma\psi - \mu \cos \mu\psi \sin \gamma\psi}{\mu \cos \mu\psi \cos \gamma\psi + \gamma \sin \mu\psi \sin \gamma\psi} \\ &\times \int_{-\psi}^{\psi} G(\theta_1) \cos \gamma\theta_1\, d\theta_1 \end{aligned} \right\} \tag{12a}$$

$$\left.\begin{aligned}C_2(\gamma,\mu,\psi) &= \frac{\mu^2-\gamma^2}{2\gamma}\\ &\times \frac{\mu\sin\mu\psi\cos\gamma\psi - \gamma\cos\mu\psi\sin\gamma\psi}{\gamma\cos\mu\psi\cos\gamma\psi + \mu\sin\mu\psi\sin\gamma\psi}\\ &\times \int_{-\psi}^{\psi} G(\theta_1)\sin\gamma\theta_1\, d\theta_1.\end{aligned}\right\} \quad (12b)$$

Equation (11) is the inversion of equation (8).

A particularly useful case occurs when

$$G(\theta) = G_0 \cos n\theta \quad (13)$$

and the explicit form of the solution is then

$$F(\theta) = \frac{G_0}{\gamma^2 - n^2}\left[(\mu^2 - n^2)\cos n\theta - (\mu^2-\gamma^2) \times \left(\frac{\mu\cos n\psi\cos\mu\psi + n\sin n\psi\sin\mu\psi}{\mu\cos\gamma\psi\cos\mu\psi + \gamma\sin\gamma\psi\sin\mu\psi}\right)\cos\gamma\theta\right]. \quad (14a)$$

When $n = \gamma = 0$, equation (14a) is an indeterminate form. One can show

$$F(\theta) = G_0\left[1 + \frac{\mu^2}{2}(\theta^2 - \psi^2) + \mu\psi\tan\mu\psi\right], \quad \gamma = n = 0. \quad (14b)$$

Another useful form occurs when $\gamma = 0$ and $n = \mu$. In such a case

$$F(\theta) = G_0/\cos\mu\psi, \ \gamma = 0, \ \mu = n. \quad (14c)$$

For compactness of presentation in the next section, we introduce the notation

$$Z_n(\gamma,\psi) = \frac{\frac{1}{2}\cos n\psi\cos\frac{1}{2}\psi + n\sin n\psi\sin\frac{1}{2}\psi}{\frac{1}{2}\cos\gamma\psi\cos\frac{1}{2}\psi + \gamma\sin\gamma\psi\sin\frac{1}{2}\psi} \quad (15)$$

which will be used in applying equation (14) to the solution of the radiative heat-transfer equations developed previously.

APPLICATIONS

The equations on the preceding pages can be used to find closed-form solutions to many problems of radiative heat balance between various forms of energy sources, and infinite shells with cross-sections forming one or more circular arcs. Four illustrative examples will be given here. The first two examples contain solutions of problems involving a shell with arbitrary arc length and oncoming diffuse radiation, finding: firstly, the heat flux when the shell temperature is held constant; and, secondly, the temperature when the shell heat flux is held constant. The second two examples contain solutions of problems involving a shell with a semicircular arc and oncoming diffuse or parallel radiation, equilibrium temperature of the shell being found when the heat conduction along it is either infinite or zero. Results for a hemisphere held to the same conditions are also given for comparative purposes.

Incident diffuse radiation, constant-temperature shell

We are concerned here with the determination of the emission and heat-transfer distributions corresponding to an imposed uniform shell temperature together with a uniform black-body source distribution specified along the chord connecting the arc of the shell. The problem is symmetrical in θ and equations (4) apply where $T(\theta_1) = \text{const.} = T_0$ and $h_2(\theta_1)$ is given by equation (7a). First casting equation (4b) in the form of (8), one finds

$$F(\theta) = B_2(\theta)$$

$$G(\theta) = e_{d_0}(1-a_2)\cos\frac{\psi}{2}\cos\frac{\theta}{2}$$

$$\mu = \tfrac{1}{2}, \qquad \gamma = \tfrac{1}{2}\sqrt{a_2}.$$

The solution is given by equation (14) where

$$n = \tfrac{1}{2}, \qquad G_0 = e_{d_0}(1-a_2)\cos\frac{\psi}{2}$$

and is

$$B_2(\theta) = e_{d_0}(1-a_2)Z_{1/2}\left(\frac{\sqrt{a_2}}{2},\psi\right)\cos\frac{\psi}{2}\cos\frac{\sqrt{a_2}}{2}\theta \quad (16)$$

which is the flux of radiation reflected from the shell at the position θ in the high average-frequency range.

Next, equation (4a) is cast in the form of (8) so

$$F(\theta) = B_1(\theta), \qquad G(\theta) = \epsilon\sigma T_0^4,$$

$$\mu = \tfrac{1}{2}, \qquad \gamma = \tfrac{1}{2}\sqrt{\epsilon}.$$

The solution is again given directly by equation (14) in which

$$n = 0, \qquad G_0 = \epsilon\sigma T_0^4.$$

Thus

$$B_1(\theta) = \sigma T_0^4 \left[1 - (1-\epsilon) Z_0 \left(\frac{\sqrt{\epsilon}}{2}, \psi\right) \cos \frac{\sqrt{\epsilon}}{2} \theta\right] \tag{17}$$

which is the emergent flux at θ in the low average-frequency range.

The total heat-transfer distribution follows from equation (5b). The result is

$$Q(\theta) = \epsilon \sigma T_0^4 \left[m + Z_0 \left(\frac{\sqrt{\epsilon}}{2}, \psi\right) \cos \frac{\sqrt{\epsilon}}{2} \theta\right] - e_{d0} \alpha_2 Z_{1/2} \left(\frac{\sqrt{\alpha_2}}{2}, \psi\right) \cos \frac{\psi}{2} \cos \frac{\sqrt{\alpha_2}}{2} \theta. \tag{18a}$$

If R is the radius of the circular arc, the integrated heat transfer per unit length of the cylinder is

$$R \int_{-\psi}^{\psi} Q(\theta)\, d\theta = 2R \left[\epsilon \sigma T_0^4 m \psi + 2\sqrt{(\epsilon)}\, \sigma T_0^4 Z_0 \left(\frac{\sqrt{\epsilon}}{2}, \psi\right) \sin \frac{\sqrt{\epsilon}}{2} \psi - 2 e_{d0} \sqrt{(\alpha_2)}\, Z_{1/2} \left(\frac{\sqrt{\alpha_2}}{2}, \psi\right) \cos \frac{\psi}{2} \sin \frac{\sqrt{\alpha_2}}{2} \psi\right]. \tag{18b}$$

Equations (16–18) supply the three quantities of principal interest, namely, the emission function, the local and the integrated heat transfer. The number of parameters (ϵ, α_2, ψ, e_{d0}), together with the variation in θ, introduces some difficulty in achieving a satisfactory graphical presentation of results. The analytic expressions involve only combinations of trigonometric functions, however, and are quickly adapted to specific applications once the geometry and range of parameters is fixed. We shall restrict ourselves here to an indication of the variation of $Z_0[\sqrt{(\epsilon)}/2, \psi] = Q(0)/\epsilon\sigma T_0^4$ (see Fig. 2). This function provides at $\theta = 0$ the local heat transfer as a function of ϵ and ψ when no external energy is oncoming ($e_{d_0} = 0$) and no energy is radiated out of the convex side. Under these conditions, the heat transfer of the constant-temperature shell is a maximum at $\theta = 0$; from equation (18a) the further variation with θ involves merely an additional cosine function as a factor. The emission function, $B_1(\theta)$, has its minimum value at $\theta = 0$ and is readily calculated from equation (17).

A non-uniformity in the value of $Q(0)/\epsilon\sigma T_0^4$ occurs at $\epsilon = 0$, $\psi = \pi$. This difficulty is not unexpected; it is known, for example, that when

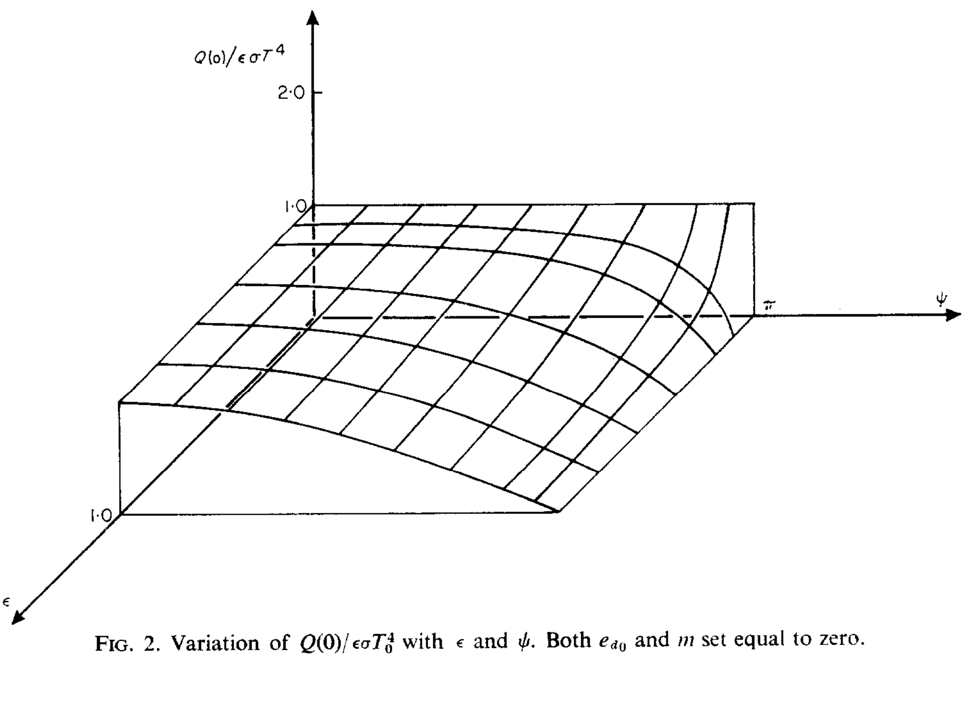

FIG. 2. Variation of $Q(0)/\epsilon\sigma T_0^4$ with ϵ and ψ. Both e_{d_0} and m set equal to zero.

$\epsilon = 0$, perfect reflectivity exists and a metastable state of radiative energy can exist within a chamber.

When the strength of the external energy source, e_{d_0}, is zero, equations (17) and (18a) yield the contrasting results:

$$B_1(\theta) = 0, \quad Q(\theta) = 0 \quad \text{when} \quad \alpha = 0,\ \psi < \pi,$$
$$B_1(\theta) = \sigma T_0^4, \quad Q(\theta) = 0 \quad \text{when} \quad \alpha > 0,\ \psi = \pi.$$

For all non-vanishing values of emissivity or absorptivity, therefore, the emission within the closed region reduces to the emission function for black-body radiation σT_0^4, as it must under conditions of thermodynamic equilibrium.

The theoretical prediction of the emission function is of especial value in the interpretation of experimental measurements when the area of escape of radiation is small, i.e. when a small slit is cut along the element of a right circular cylinder whose wall is held at a uniform temperature. Let $\psi = \pi - \delta$ where 2δ is the angle subtended by the slit at the center of the cylinder. If radiation from the external environment can be ignored, equation (17) gives the emission from within the cavity at the wall temperature T_0. For very small δ this reduces to

$$B_1(\theta) = \sigma T_0^4 \left[1 - \frac{(1-\epsilon)\delta \cos[\sqrt{(\epsilon)}/2]\,\theta}{2\sqrt{(\epsilon)}\sin[\sqrt{(\epsilon)}\pi/2]}\right]. \quad (19a)$$

Similarly, the integrated heat transfer per unit length of cylinder reduces to

$$R\int_{-(\pi-\delta)}^{\pi-\delta} Q\, d\theta = 2R\delta\sigma T_0^4\left(1 - \frac{\delta\sqrt{\epsilon}}{2}\cot\frac{\pi\sqrt{\epsilon}}{2}\right). \quad (19b)$$

Incident diffuse radiation, constant heat transfer

We are concerned here with the determination of the temperature distribution corresponding to an imposed uniform heat transfer along a circular arc. Let us further consider only the case $m = 0$ for which there is no radiation away from the convex side. From equations (6a) and (6b), it is apparent that the solution depends upon two simultaneous integral equations. However, equation (6b) is independent of (6a) and, in fact, its solution has already been found for incident diffuse radiation and presented in equation (16). Substituting equations (16) and (7a) into equation (6a) and identifying terms with those in the general equation, equation (8), one finds

$$F(\theta) = \epsilon\sigma T^4 - (1-\epsilon)Q$$

$$G(\theta) = \epsilon Q + \frac{e_{d_0}\alpha_2\cos(\psi/2)}{1-\alpha_2}\left[(1-\epsilon)\cos\frac{\theta}{2} + (\epsilon-\alpha_2)Z_{1/2}\left(\frac{\sqrt{\alpha_2}}{2},\psi\right)\cos\frac{\sqrt{\alpha_2}}{2}\theta\right]$$

$$\mu = \tfrac{1}{2}, \qquad \gamma = 0.$$

If Q is a constant equal to Q_0, equations (13) and (14a–c) can be used to show

$$F(\theta) = \epsilon Q_0\left[1 + \frac{1}{8}(\theta^2 - \psi^2) + \frac{1}{2}\psi\tan\frac{\psi}{2}\right] + \frac{e_{d_0}\alpha_2(1-\epsilon)\cos(\psi/2)}{1-\alpha_2}\left[\frac{1}{\cos(\psi/2)}\right] + \frac{e_{d_0}\alpha_2(\epsilon-\alpha_2)\cos(\psi/2)}{1-\alpha_2}Z_{1/2}\left(\frac{\sqrt{\alpha_2}}{2},\psi\right) \times \left[\frac{\alpha_2-1}{\alpha_2}\cos\frac{\sqrt{\alpha_2}}{2}\theta + \frac{1}{\alpha_2}Z_{\sqrt{(\alpha)}/2}(0,\psi)\right].$$

Since

$$Z_{1/2}\left(\frac{\sqrt{\alpha}}{2},\psi\right)Z_{\sqrt{(\alpha)}/2}(0,\psi) = \frac{1}{\cos(\psi/2)},$$

one finds, after combining terms,

$$\left.\begin{aligned}\epsilon\sigma T^4(\theta) &= Q_0 + \frac{\epsilon}{2}Q_0\left[\psi\tan\frac{\psi}{2} + \frac{1}{4}(\theta^2-\psi^2)\right] + e_{d_0}\left[\alpha_2 - (\epsilon-\alpha_2) \times Z_{1/2}\left(\frac{\sqrt{\alpha_2}}{2},\psi\right)\cos\frac{\psi}{2}\cos\frac{\sqrt{\alpha_2}}{2}\theta\right].\end{aligned}\right\} \quad (20)$$

It is apparent that, when there is no external energy source, i.e. when $e_{d_0} = 0$, the function $\epsilon\sigma T^4(\theta)$ associated with uniform heat transfer has its minimum value at the point of symmetry $\theta = 0$ and its maximum value at $\theta = \psi$. The function $\epsilon\sigma T^4(\theta)/Q_0$ increases quadratically with θ from its low point and achieves the maximum value $\epsilon\sigma T^4(0)/Q_0 + \epsilon\psi^2/8$. In Fig. 3 the dependence of $\epsilon\sigma T^4(0)/Q_0$ on ϵ and ψ is indicated. It is to be noted that, as in Fig. 2, a non-uniformity appears at $\epsilon = 0$, $\psi = \pi$. For non-vanishing values of emission, infinite temperature is predicted when closure is complete, but the results are for the equilibrium case, so an infinite energy input would also be required in such a case.

conditions $m = 1$ and the total heat transfer must be zero, that is

$$R \int_{-\psi}^{\psi} Q(\theta)\, d\theta = 0. \tag{21}$$

Under this condition, and with the simplification

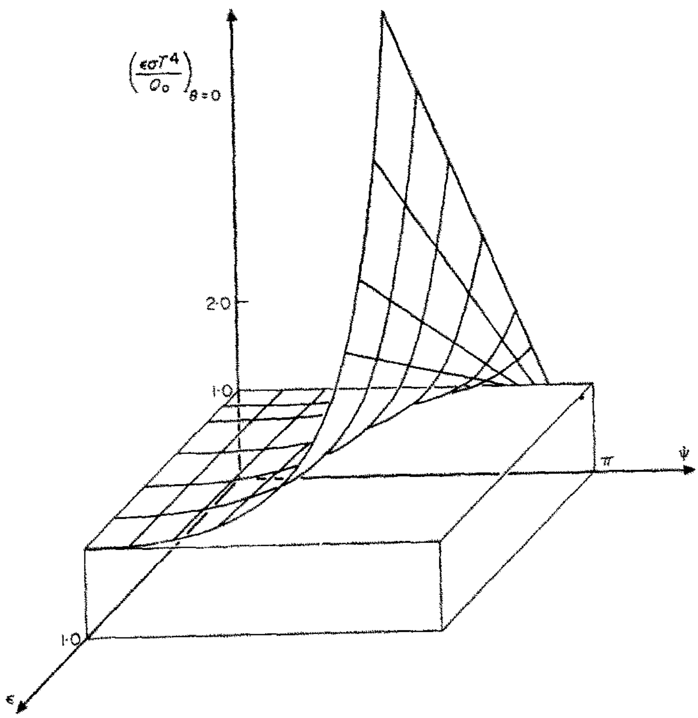

FIG. 3. Variation of $(\epsilon\sigma T^4/Q_0)_{\theta=0}$ with ϵ and ψ; see equation (20).

Thermal radiation shield with infinite conductivity

When the conductivity of the shell is infinite, its temperature is uniform and the two equations for the high and low average-frequency, thermal-radiation flux, equations (4a) and (4b), can be solved independently, just as in the first example considered. In fact, if the oncoming radiation is diffuse, the solution in terms of heat transfer is given immediately by equation (18a). The physical character of the problem has changed somewhat, however. Here the surface is assumed to be a thin shell, with a semicircular cross-section, radiating to a very low temperature environment (or back to a black-body source, if the incoming radiation is diffuse), and receiving energy on the concave side from a source with a relatively high effective temperature. Under such caused by setting $\psi = \pi/2$, equation (18b) yields

$$\frac{\sigma T_E^4}{e_{d_0}} = \sqrt{\frac{a_2}{\epsilon}}\left[1 + \frac{\pi\sqrt{\epsilon}}{4}\left(\cot\frac{\pi\sqrt{\epsilon}}{4} + \sqrt{\epsilon}\right)\right]^{-1} \times \frac{\cot[\pi\sqrt{(\epsilon)}/4] + \sqrt{\epsilon}}{\cot[\pi\sqrt{(a_2)}/4] + \sqrt{a_2}} \tag{22}$$

for the equilibrium shell temperature T_E. Following exactly the same procedure, but assuming parallel oncoming radiation [equation (7b) for $h_2(\theta)$], one can show

$$\left[\frac{\sigma T_E^4}{e_{s_0}}\right]_{\text{parallel}} = \left[\frac{\sigma T_E^4}{e_{d_0}}\right]_{\text{diffuse}} \times \left[\frac{1}{2}\left(1 + \frac{3\sqrt{(a_2)}\cot[\pi\sqrt{(a_2)}/4]}{4 - a_2}\right)\right]. \tag{23}$$

It is to be noted that the only difference between the equilibrium temperatures for the diffuse and parallel radiation is the term within the brackets in equation (23). This term is a function only of a_2, the absorptivity coefficient for the high (effective) temperature radiation. It is very insensitive to a_2, however, varying only from 0·977 to 1 for the range $a_2 = 0\text{–}1$, respectively. In the case of infinite conductivity, therefore, the shield equilibrium temperature based on equations (6) for both parallel and diffuse impinging radiation is given, with an error of less than 2·3 per cent, by equation (22).

Further approximations in equation (22) serve to indicate the range of equilibrium temperature. The inequality

$$\frac{x}{2} \leq \left(\cot\frac{\pi x}{4} + x\right)^{-1} \leq \frac{\pi x}{4}, \quad 0 \leq x \leq 1$$

can be used together with equation (22) rewritten in the form

$$\frac{\sigma T_E^4}{e_{d_0}} = \frac{1}{2}\sqrt{\frac{a_2}{\epsilon}} \times \frac{\{\cot[\pi\sqrt{(a_2)}/4] + \sqrt{a_2}\}^{-1}}{[\pi\sqrt{(\epsilon)}/4] + \{\cot[\pi\sqrt{(\epsilon)}/4] + \sqrt{\epsilon}\}^{-1}}.$$

It follows that

$$\frac{a_2}{2\pi\epsilon} \leq \frac{\sigma T_E^4}{e_{d_0}} \leq \frac{a_2}{\epsilon}\,\frac{\pi}{2(2+\pi)}$$

or, alternatively,

$$0{\cdot}63\left(\frac{a_2 e_{d_0}}{\epsilon\sigma}\right)^{1/4} \leq T_E \leq 0{\cdot}744\left(\frac{a_2 e_{d_0}}{\epsilon\sigma}\right)^{1/4}.$$

Figure 4 shows a typical variation of the equilibrium temperature with a_2 for a fixed ϵ. One can show that the result for a hemispherical shell with infinite conductivity is

$$\left[\frac{\sigma T_E^4}{e_{d_0}}\right]_{\text{diffuse}} = \left[\frac{\sigma T_E^4}{e_{s_0}}\right]_{\text{parallel}} = \frac{a_2}{\epsilon}\,\frac{1+\epsilon}{1+a_2}\,\frac{1}{2+\epsilon}. \quad (24)$$

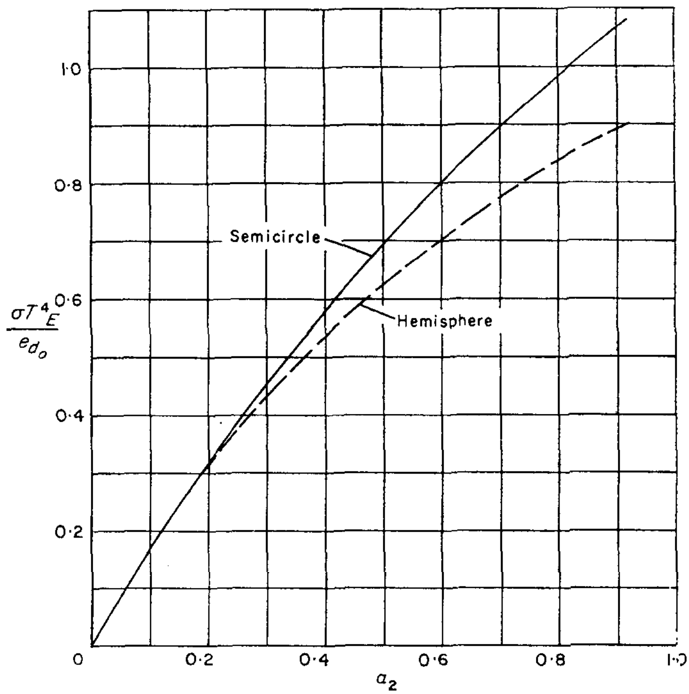

FIG. 4. Equilibrium temperatures on hemispheres and two-dimensional cylinders with circular-arc sections having absorptivity coefficient a_2 for oncoming diffuse radiation; infinite conductivity, $\epsilon = 0{\cdot}3$.

This result is also given in Fig. 4 and shows that there is little practical difference in equilibrium temperature between the semicircular cylinder and the hemisphere, except for high values of α_2. This is true for all ϵ.

Thermal radiation shield with zero conductivity

In the limiting case of zero conductivity, no heat is transferred along the circular arc. Hence, the condition for an equilibrium energy balance (under the assumptions previously mentioned) between a shield and a high temperature source is given by equations (6a) and (6b) in which $m = 1$ and $Q = 0$.

Solutions to equation (6b) follow exactly as in the previous examples, and equation (6a) reduces, for $Q = 0$, to a form identical to equation (8) in which $F(\theta)$ represents $(2 - \epsilon)\epsilon\sigma T^4$. Solutions for diffuse and parallel impinging radiation, therefore, can easily be obtained, and when $\psi = \pi/2$, they take the form

$$\frac{\sigma T_E^4}{e_{d_0}} = B_1(\alpha_2, \epsilon) \cos \frac{1}{2}\sqrt{\left(\frac{\epsilon}{2}\right)}\,\theta - B_2(\alpha_2, \epsilon) \cos \frac{\sqrt{\alpha_2}}{2}\theta \quad (25)$$

where

$$B_1(\alpha_2, \epsilon) = \alpha_2 \left[2(2\alpha_2 - \epsilon)\left(\cos\frac{\pi}{4}\sqrt{\frac{\epsilon}{2}} + \sqrt{\frac{\epsilon}{2}}\sin\frac{\pi}{4}\sqrt{\frac{\epsilon}{2}}\right)\right]^{-1}$$

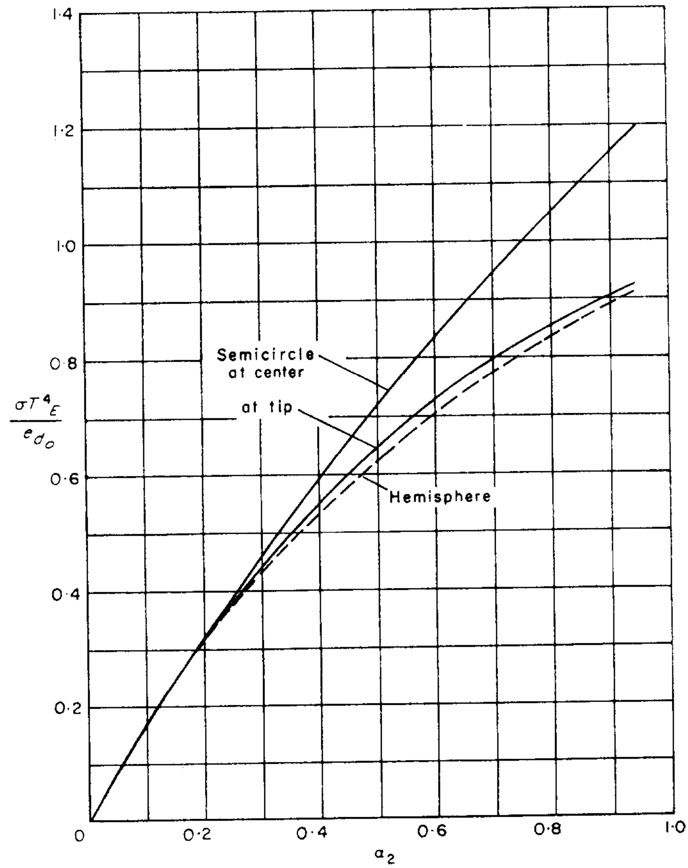

FIG. 5. Equilibrium temperatures on hemispheres and two-dimensional cylinders with circular-arc sections having absorptivity coefficient α_2 for oncoming diffuse radiation; zero conductivity, $\epsilon = 0{\cdot}3$.

$$B_2(a_2, \epsilon) = a_2(\epsilon - a_2)\left[\epsilon(2a_2 - \epsilon) \times \left(\cos\frac{\pi\sqrt{a_2}}{4} + \sqrt{(a_2)}\sin\frac{\pi\sqrt{a_2}}{4}\right)\right]^{-1}$$

and

$$\frac{\sigma T_E^4}{e_{s_0}} = \frac{3a_2(4-\epsilon)\cos\theta}{\epsilon(4-a_2)(8-\epsilon)} + \frac{2(2-\epsilon)}{8-\epsilon}B_1(a_2, \epsilon)\cos\frac{1}{2}\sqrt{\left(\frac{\epsilon}{2}\right)}\theta - \frac{2(1-a_2)}{4-a_2}B_2(a_2, \epsilon)\cos\frac{\sqrt{a_2}}{2}\theta \quad (26)$$

respectively. Similarly, one can show that a hemispherical shell having zero conductivity has equilibrium temperature distributions given by

$$\frac{\sigma T_E^4}{e_{d_0}} = \frac{a_2}{\epsilon}\frac{1+\epsilon}{1+a_2}\frac{1}{2+\epsilon} \quad (27)$$

and

$$\left[\frac{\sigma T_E^4}{e_{s_0}}\right]_{\text{parallel}} = \left[\frac{\sigma T_E^4}{e_{d_0}}\right]_{\text{diffuse}} + \tfrac{1}{2}(\cos\theta - \tfrac{1}{2}) \quad (28)$$

for the diffuse and parallel radiation cases, respectively.

These results are not similar, as they were in the previous example, for the two types of oncoming radiation considered. This is illustrated for the case $\epsilon = 0{\cdot}3$ in Figs. 5 and 6. When the conductivity is zero the temperature is no longer uniform, but, as illustrated in Fig. 5, it does not

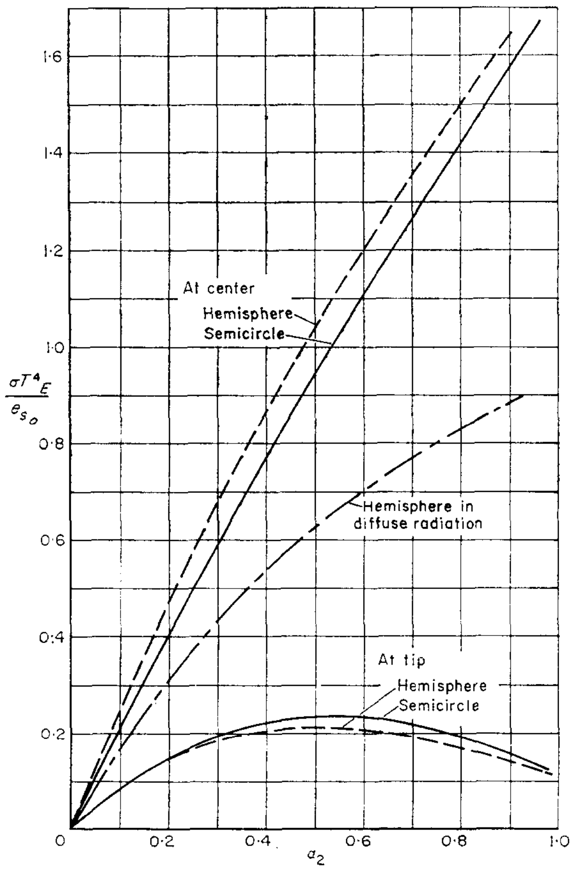

FIG. 6. Equilibrium temperatures on hemispheres and two-dimensional cylinders with circular-arc sections having absorptivity coefficient a_2 for oncoming parallel radiation; zero conductivity, $\epsilon = 0{\cdot}3$.

vary greatly when the impinging radiation is diffuse. Comparing with Fig. 4, one sees that the average equilibrium temperature for the diffuse, zero-conductivity case is not greatly different from the constant equilibrium temperature for either the diffuse or parallel, infinite-conductivity case. (The results for the hemisphere are the same in both cases.) This result is qualitatively true for all $\epsilon > 0{\cdot}1$.

The temperature distribution caused by parallel source radiation for both the cylinder and hemisphere is greatly different for the zero- and infinite-conductivity cases. Fig. 6 provides a measure of the temperature at the edge and at the center of cylinders and hemispheres for the parallel, zero-conductivity case. The temperature at the center is relatively much higher. The results for the diffuse radiation source just about average the two extremes. Again, these statements are qualitatively true for all ϵ.

REFERENCE

1. M. Jakob, *Heat Transfer* Vol. 2. John Wiley, New York (1957).

Résumé—Le rayonnement diffus d'enceintes infinies à section droite circulaire est étudié dans les cas où les sources de rayonnement diffus ou parallèle sont extérieures.

Les équations intégrales sont dérivées dans les conditions d'une analyse modifiée du corps gris et les inversions données sous une forme fermée.

Des applications particulières donnent: l'échange thermique local correspondant à une température d'enceinte constante, la température locale correspondant à un échange thermique constant, et les prévisions des températures d'équilibre, quand l'enceinte est un champ thermique. Ces calculs sont comparés aux calculs analogues effectués pour des écrans hémisphériques.

Zusammenfassung—Die diffuse Strahlung von unendlich langen, halbkreisförmig gebogenen Schalen wird analysiert, wobei auch äussere Quellen als diffuse oder parallele Strahler berücksichtigt sind. Die massgeblichen Integralgleichungen sind für einen modifizierten grauen Körper abgeleitet und ihre Umkehrungen in geschlossener Form angegeben. Spezielle Ableitungen ergeben den örtlichen Wärmeübergang bei konstanter Wandtemperatur, die örtliche Temperatur bei konstantem Wärmeübergang und die Gleichgewichtstemperatur, wenn die Schale als thermischer Schild betrachtet wird. Ähnliche Berechnungen für Kugelschalen dienten als Vergleich.

Аннотация—Анализируется диффузное излучение с бесконечных оболочек, имеющих поперечные сечения в виде дуг окружностей, для случаев внутренних полей источников рассеянного или направленного излучения. Выведены исходные интегральные уравнения для условий, соответствующих модифицированному соотношению излучения серого тела, и приведены обращения в замкнутой форме. Частные применения дают возможность определить локальный теплоперенос при постоянной температуре оболочки, локальную температуру, соответствующую постоянному теплопереносу, и предсказать равновесные температуры для случая, когда оболочка представляет собой тепловой экран. Проведены сравнения с подобными вычислениями для полусферических экранов.